

Signature of (axial)vector operators in $B_c \rightarrow D_s^{(*)} \mu^+ \mu^-$ decays

Manas Kumar Mohapatra^{a,*}, Ajay Kumar Yadav^{b,†} and Suchismita Sahoo^{b‡}

School of Physics, University of Hyderabad, Hyderabad-500046, India ^a

Department of Physics, Central University of Karnataka, Kalaburagi-585367, India ^b

Abstract

The persistent anomalies observed in B mesons related to $b \rightarrow s\mu^+\mu^-$ transitions point to the potential for new physics beyond the Standard Model. To explore this further, we conduct an analysis of the exclusive semileptonic decays $B_c \rightarrow D_s^{(*)} \mu^+ \mu^-$ within an effective field theory formalism. We perform a global fit to new (axial)vector couplings using the current experimental data for $b \rightarrow s\mu^+\mu^-$ transitions. We compute the branching ratios and physical observables such as forward-backward asymmetries, lepton polarization asymmetries, form factor independent observables for $B_c \rightarrow D_s^{(*)} \mu^+ \mu^-$, both within the Standard Model and in new physics scenarios. Additionally, we examine the existence of lepton flavor universality violation in the $B_c \rightarrow D_s^{(*)} \ell^+ \ell^-$ process.

*Electronic address: manasmohapatra12@gmail.com

†Electronic address: yadavajaykumar286@gmail.com

‡Electronic address: suchismita8792@gmail.com

I. INTRODUCTION

The Standard Model (SM) of particle physics has proven remarkably successful in describing the interactions of elementary particles and making precise predictions across a wide range of phenomena. However, despite its accomplishments, the SM falls short in explaining several fundamental aspects of the Universe, such as dark matter, dark energy, neutrino mass, and the matter-antimatter asymmetry. To address these unresolved questions, physicists have devoted considerable effort to the search for new physics (NP). One avenue of exploration involves probing rare decays of B mesons, particularly those involving flavor changing neutral (FCNC) transitions like $b \rightarrow s/d l^+l^-$ modes [1–16] and flavor changing charged current (FCCC) transitions such as $b \rightarrow cl\nu_l$ [17–29], to uncover deviations from SM predictions indicating the presence of NP. The $b \rightarrow sll$ transitions have garnered significant attention as they could reveal signs of new physics. Particularly noteworthy are the lepton non-universality (LNU) observables $R_{K^{(*)}}$, which are defined as the ratios of branching fractions $\mathcal{B}(B \rightarrow K^{(*)}\mu\mu)$ to $\mathcal{B}(B \rightarrow K^{(*)}ee)$. Recent measurements, updated by the LHCb Collaboration [5, 30],

$$\text{low-}q^2 \left\{ \begin{array}{l} R_K = 0.994^{+0.090}_{-0.082}(\text{stat})^{+0.029}_{-0.027}(\text{syst}) \\ R_{K^*} = 0.927^{+0.093}_{-0.087}(\text{stat})^{+0.036}_{-0.035}(\text{syst}) \end{array} \right\}, \quad (1)$$

$$\text{central-}q^2 \left\{ \begin{array}{l} R_K = 0.949^{+0.042}_{-0.041}(\text{stat})^{+0.022}_{-0.022}(\text{syst}) \\ R_{K^*} = 1.027^{+0.072}_{-0.068}(\text{stat})^{+0.027}_{-0.026}(\text{syst}) \end{array} \right\}, \quad (2)$$

are almost consistent with the SM predictions with a disagreement of 0.2σ . Besides these parameters, a notable 3.3σ deviation [1, 3, 4, 31–34] from SM predictions has been observed in the measurement of P'_5 of $B \rightarrow K^*\mu\mu$ process. The branching ratio of the $B_s \rightarrow \phi\mu^+\mu^-$ decay mode demonstrates a significant 3.3σ deviation within the momentum transfer range of $q^2 \in [1.1, 6.0]$ GeV 2 [35–39]. Furthermore, measurements of $R_{K_S^0}$ and $R_{K^{*+}}$ [40–42] ratios disagree with SM predictions at levels of 1.4σ and 1.5σ , respectively. Although these intriguing discrepancies may be due to statistical fluctuations or underestimated theory uncertainties, they do not entirely rule out the possibility of new physics. This underscores the need for ongoing investigation to understand the dynamics and potential new physics effects in $b \rightarrow sll$ transitions.

Hints of new physics in the $B \rightarrow K^{(*)}l^+l^-$ decay modes may also be reflected in several other decays. To investigate this, we examine the $B_c \rightarrow D_s^{(*)}\mu^+\mu^-$ decays mediated by

$b \rightarrow s\mu^+\mu^-$ neutral current transitions within the framework of the effective field theory (EFT), including NP in Wilson Coefficients. Previous studies have investigated the $B_c \rightarrow D_s^{(*)}\mu^+\mu^-$ decays within the framework of the SM. These decay modes have been studied using several new theoretical approaches, including the covariant confined quark model[43, 44], the light-front quark model [45], QCD sum rules [46–48], and the relativistic quark model [49–51]. Moreover, beyond the Standard Model, these decays have been studied in both model independent [52–54] and model-dependent frameworks, including the supersymmetric models[55], leptoquarks and Z' model[51, 56]. In this study, we scrutinize the impact of (axial)vector couplings on the branching ratios and physical observables of $B_c \rightarrow D_s^{(*)}\mu^+\mu^-$ processes. We perform a global fit to the new couplings for both 1D and 2D scenarios by using the current experimental data on $b \rightarrow s\mu^+\mu^-$.

The paper is structured in the following manner: In section II, we recapitulate the Effective Hamiltonian associated with semileptonic decays involving $b \rightarrow sl^+l^-$ quark level transitions. Section III discusses the numerical fit to the new (axial)vector Wilson coefficients for both 1D and 2D scenarios. The implications of new constrained parameters on $B_c \rightarrow D_s^{(*)}\mu^+\mu^-$ is presented in section IV and V, respectively. Finally, we discuss the summary and conclusion in section VI.

II. EFFECTIVE HAMILTONIAN

The general effective Hamiltonian for rare semileptonic $b \rightarrow s\mu^+\mu^-$ transition is given as [57–59],

$$\mathcal{H}_{eff} = -\frac{4G_F}{\sqrt{2}}V_{tb}V_{ts}^*\left[C_7^{eff}\mathcal{O}_7 + C_7'\mathcal{O}_7' + \sum_{i=9,10,P,S}\left((C_i + C_i^{NP})\mathcal{O}_i + C_i'^{NP}\mathcal{O}_i'\right)\right], \quad (3)$$

where $G_F = 1.16637 \times 10^{-5} \text{ GeV}^{-2}$ is the Fermi coupling constant, V_{ij} represents the Cabibbo-Kobayashi-Maskawa (CKM) matrix elements. Here, the four fermion operators $\mathcal{O}_i^{(i)}$, where

$i = 7, 9, 10, S, P$, are given as

$$\begin{aligned}\mathcal{O}_7 &= \frac{e}{16\pi^2} m_b (\bar{s}\sigma_{\mu\nu}P_R b) F^{\mu\nu}, & \mathcal{O}'_7 &= \frac{e}{16\pi^2} m_b (\bar{s}\sigma_{\mu\nu}P_L b) F^{\mu\nu} \\ \mathcal{O}_9 &= \frac{e^2}{16\pi^2} (\bar{s}\gamma_\mu P_L b)(\bar{\mu}\gamma^\mu\mu), & \mathcal{O}'_9 &= \frac{e^2}{16\pi^2} (\bar{s}\gamma_\mu P_R b)(\bar{\mu}\gamma^\mu\mu), \\ \mathcal{O}_{10} &= \frac{e^2}{16\pi^2} (\bar{s}\gamma_\mu P_L b)(\bar{\mu}\gamma^\mu\gamma_5\mu), & \mathcal{O}'_{10} &= \frac{e^2}{16\pi^2} (\bar{s}\gamma_\mu P_R b)(\bar{\mu}\gamma^\mu\gamma_5\mu), \\ \mathcal{O}_S &= \frac{e^2}{16\pi^2} m_b (\bar{s}P_R b)(\bar{\mu}\mu), & \mathcal{O}'_S &= \frac{e^2}{16\pi^2} m_b (\bar{s}P_L b)(\bar{\mu}\mu), \\ \mathcal{O}_P &= \frac{e^2}{16\pi^2} m_b (\bar{s}P_R b)(\bar{\mu}\gamma_5\mu), & \mathcal{O}'_P &= \frac{e^2}{16\pi^2} m_b (\bar{s}P_L b)(\bar{\mu}\gamma_5\mu),\end{aligned}$$

where $P_{R,L} = (1 \pm \gamma_5)/2$ are the chirality operators and $C_i^{(\prime)}$'s are the corresponding Wilson coefficients[60]. The SM does not include contributions from primed Wilson coefficients or (pseudo)scalar coefficients. These coefficients only appear in theories beyond the Standard Model.

III. FITTING NEW COUPLINGS TO $b \rightarrow s\mu\mu$ TRANSITIONS

To address the observed discrepancies, we initiate our analysis with a model-independent approach, thoroughly examining the data and focusing on observables in $b \rightarrow s\mu^+\mu^-$ decays that exhibit deviations from SM predictions. Particular attention is given to scenarios where potential new physics contributions could impact the vector Wilson coefficients $C_9^{(\prime)\text{NP}}$ and the axial-vector Wilson coefficients $C_{10}^{(\prime)\text{NP}}$. The $b \rightarrow s\mu^+\mu^-$ observables incorporated into our global fit analyses are outlined below.

- **Branching Ratios:** The LHCb collaboration updated the experimental value of the $\mathcal{B}(B_s \rightarrow \mu^+\mu^-)$ at Moriond 2021 [61]. The measured value of $3.09_{-0.43-0.11}^{+0.46+0.15} \times 10^{-9}$ closely aligns with the previous world average [62], derived from the combined measurements of the ATLAS [63], CMS [64], and LHCb [65] Collaborations. We also consider the branching ratios for $B^0 \rightarrow K^{*0}\mu^+\mu^-$, $B^+ \rightarrow K^{*+}\mu^+\mu^-$, $B^0 \rightarrow K^0\mu^+\mu^-$, and $B^+ \rightarrow K^+\mu^+\mu^-$ [66, 67], evaluated across different q^2 bins. Additionally, we update our fit with the measured branching fractions for $B_s \rightarrow \phi\mu^+\mu^-$ provided by LHCb, across a range of q^2 interval [38].
- **Angular Observables for $B^0 \rightarrow K^{*0}\mu^+\mu^-$:** We include measurements of the forward-backward asymmetry A_{FB} [1], longitudinal polarization fraction F_L , CP-

averaged observables $S_{i=3,4,5,7,8,9}$, CP asymmetries $A_{i=3,4,5,7,8,9}$ and the form factor independent observables $P_1 - P'_8$ [4], across various q^2 intervals: [0.10, 0.98], [1.1, 2.5], [2.5, 4.0], [4.0, 6.0] and [1.1, 6.0].

- **Angular Observables for $B^+ \rightarrow K^{*+} \mu^+ \mu^-$:** In addition to the optimized observables $P_1 - P'_8$, the LHCb collaboration [3] has delivered a comprehensive measurement of angular observables for this decay mode, covering a range of q^2 intervals.

We now proceed with the analysis of new physics operators, specifically $\mathcal{O}_9^{(\prime)NP}$ and $C_{10}^{(\prime)NP}$, examining both one-dimensional (1D) and two-dimensional (2D) scenarios, where new physics is considered solely within the μ -sector. In this study, we employ all the observables discussed previously and conduct our analysis using the `flavio` package [68]. A complete analysis of the fit results derived from the $b \rightarrow s\mu\mu$ data is presented in Table I for one-dimensional scenarios and Table II for two-dimensional scenarios. The scenarios for all possible new physics couplings are labeled from S-I to S-XI. Additionally, we report the best-fit values along with their 1σ uncertainties, the pull = $\sqrt{\chi_{\text{SM}}^2 - \chi_{\text{best-fit}}^2}$ values, and the p-values (%). We constrain the new physics parameter space and illustrate the 3σ allowed region from the $b \rightarrow s\mu^+\mu^-$ data, highlighted in green. The regions corresponding to 1σ to 3σ confidence levels are depicted in progressively lighter shades of green, as shown in Fig. 1. We find that the 1D scenario labeled S-VI yields the highest pull value, while in the 2D context, the optimal pull value is obtained for the S-I scenario.

IV. ANALYSIS OF $B_c \rightarrow D_s \mu^+ \mu^-$ DECAY

After establishing the best-fit values and 1σ uncertainties for the new (axial)vector coefficients, we further analyze their impact on the branching ratio and angular observables of the $B_c \rightarrow D_s \mu^+ \mu^-$ decay mode. This investigation seeks to reveal how these coefficients influence the decay dynamics, offering a deeper insight into the potential contributions of new physics to this process. The q^2 differential decay rate for $B_c \rightarrow D_s \mu^+ \mu^-$ process in the presence of new physics is given as [69]

$$\frac{d\Gamma(B_c \rightarrow D_s \mu^+ \mu^-)}{dq^2} = 2 a_l(q^2) + \frac{2}{3} c_l(q^2), \quad (4)$$

TABLE I: Best-fit values [1σ], pull, p-value(%) of different single Wilson coefficient NP scenarios in $b \rightarrow s\mu^+\mu^-$ transitions.

Scenario	Coefficient	Best-fit value [1σ]	Pull	p-value (%)
S - I	C_9^{NP}	-1.227 [${}^{+0.959}_{-1.363}$]	4.665	46.0
S - II	C_{10}^{NP}	0.456 [${}^{+0.555}_{-0.252}$]	2.823	22.0
S - III	C'_9^{NP}	0.082 [${}^{+0.353}_{-0.252}$]	0.261	14.0
S - IV	C'_{10}^{NP}	-0.134 [${}^{-0.050}_{-0.252}$]	1.085	13.0
S - V	$C_9^{\text{NP}} = C_{10}^{\text{NP}}$	0.023 [${}^{+0.250}_{-0.050}$]	0.158	15.0
S - VI	$C_9^{\text{NP}} = -C_{10}^{\text{NP}}$	-0.971 [${}^{-0.757}_{-1.161}$]	4.921	53.0
S - VII	$C'_9^{\text{NP}} = C'_{10}^{\text{NP}}$	-0.135 [${}^{-0.052}_{-0.251}$]	1.003	14.0
S - VIII	$C'_9^{\text{NP}} = -C'_{10}^{\text{NP}}$	0.109 [${}^{+0.147}_{-0.048}$]	1.046	15.0
S - IX	$C_9^{\text{NP}} = -C'_9^{\text{NP}}$	-0.835 [${}^{-0.656}_{-0.959}$]	3.993	31.0
S - X	$C_9^{\text{NP}} = -C_{10}^{\text{NP}} = -C'_9^{\text{NP}} = -C'_{10}^{\text{NP}}$	-0.374 [${}^{-0.254}_{-0.451}$]	3.067	24.0
S - XI	$C_9^{\text{NP}} = -C_{10}^{\text{NP}} = C'_9^{\text{NP}} = -C'_{10}^{\text{NP}}$	-0.281 [${}^{-0.150}_{-0.454}$]	2.415	20.0

where, $a_l(q^2)$ and $c_l(q^2)$ are defined as

$$a_l(q^2) = N_{D_s} \left[q^2 |F_p|^2 + \frac{\lambda(m_{B_c}^2, m_{D_s}^2, q^2)}{4} (|F_A|^2 + |F_V|^2) + 4m_l^2 m_{B_c}^2 |F_A|^2 + 2m_l(m_{B_c}^2 - m_{D_s}^2 + q^2) \operatorname{Re}(F_p F_A^*) \right],$$

$$c_l(q^2) = -N_{D_s} \frac{\lambda(m_{B_c}^2, m_{D_s}^2, q^2) \beta_l^2}{4} (|F_A|^2 + |F_V|^2),$$

with

$$N_{D_s} = \frac{G_F^2 \alpha_e^2 |V_{tb} V_{ts}^*|^2}{2^9 \pi^5 m_{B_c}^3} \beta_l \sqrt{\lambda(m_{B_c}^2, m_{D_s}^2, q^2)},$$

the kinematic component $\lambda(a, b, c) = a^2 + b^2 + c^2 - 2(ab + bc + ca)$ and the mass correction factor $\beta_l = \sqrt{1 - \frac{4m_l^2}{q^2}}$. Here the $F_{P,V,A}$ functions are defined as

$$F_P = -m_l C_{10} \left[f_+ - \frac{m_{B_c}^2 - m_{D_s}^2}{q^2} (f_0 - f_+) \right],$$

$$F_V = C_9^{\text{eff}} f_+ + \frac{2m_b}{m_{B_c} + m_{D_s}} C_7^{\text{eff}} f_T,$$

$$F_A = C_{10} f_+.$$

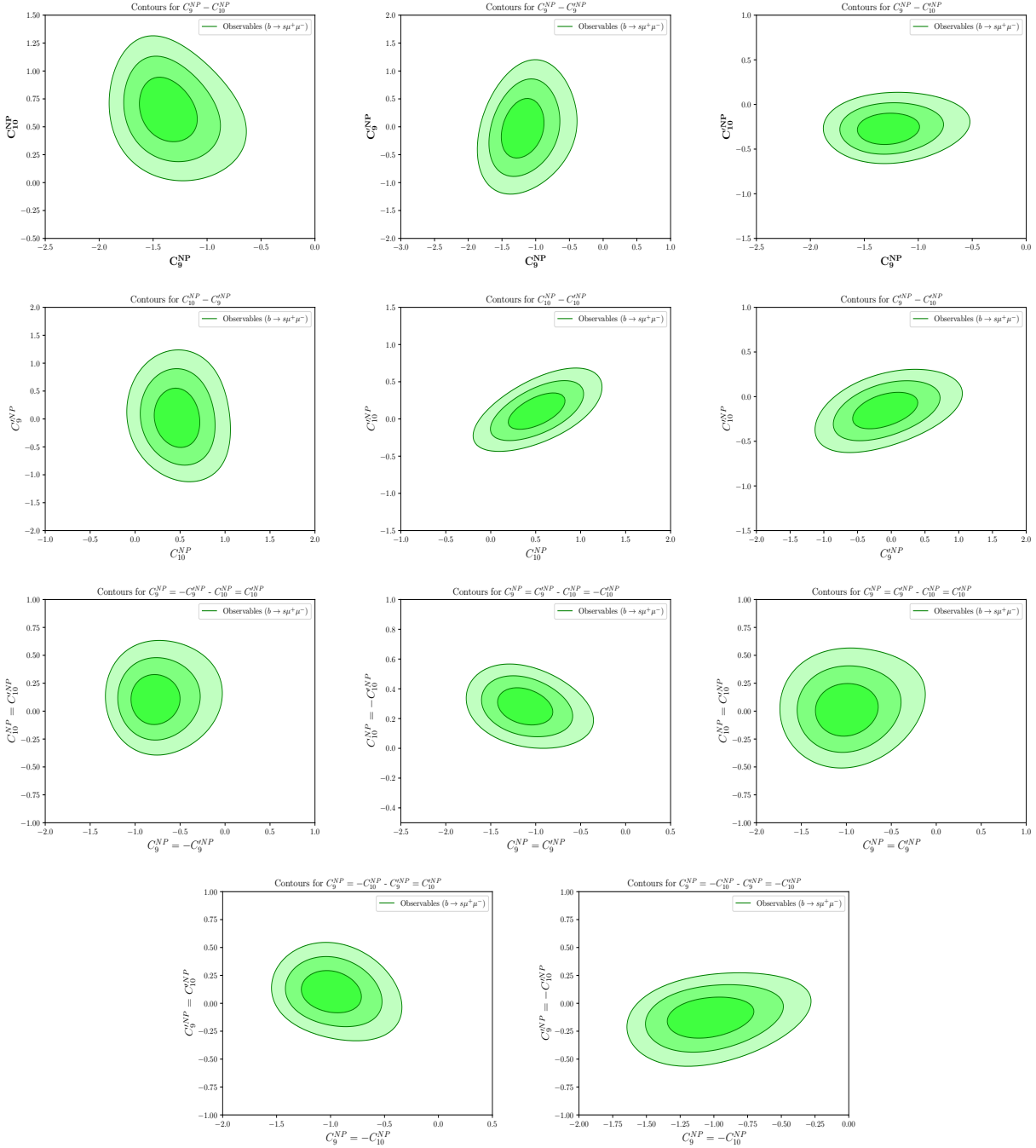


FIG. 1: Allowed parameter space for new physics scenarios of various observables associated with the $b \rightarrow s \mu^+ \mu^-$ transitions.

Using the required input parameters from PDG site[70] and the relativistic quark model form factor for the $B_c \rightarrow D_s$ transition from ref.[49], we investigate the branching ratio and LNU parameter of $B_c \rightarrow D_s \mu^+ \mu^-$ process in the SM and in the presence of new (axial)vector coefficients. Based on the 1σ allowed ranges of new coefficients in various 1D and 2D

TABLE II: Best-fit values [1σ], pull, p-value(%) for different combinations of two Wilson coefficient NP scenarios in $b \rightarrow s\mu^+\mu^-$ transitions.

Scenario	Coefficient	Best fit value [1σ]	Pull	p-value (%)
S - I	$(C_9^{\text{NP}}, C_{10}^{\text{NP}})$	$(-1.398[-1.219, 0.694[0.855]], 0.694[0.480])$	5.961	67.0
S - II	$(C_9^{\text{NP}}, C'_9^{\text{NP}})$	$(-1.206[-0.988, -0.020[0.325]], -0.020[-0.367])$	4.640	47.0
S - III	$(C_9^{\text{NP}}, C'_{10}^{\text{NP}})$	$(-1.269[-1.079, -0.306[-0.158]], -0.306[-0.390])$	5.239	53.0
S - IV	$(C_{10}^{\text{NP}}, C'_9^{\text{NP}})$	$(0.516[0.634], -0.050[-0.333])$	3.106	16.0
S - V	$(C_{10}^{\text{NP}}, C'_{10}^{\text{NP}})$	$(0.469[0.680], 0.101[-0.237])$	2.565	20.0
S - VI	$(C'_9^{\text{NP}}, C'_{10}^{\text{NP}})$	$(-0.033[0.283], -0.133[-0.008])$	1.059	13.0
S - VII	$(C_9^{\text{NP}} = -C'_9^{\text{NP}}, C_{10}^{\text{NP}} = C'_{10}^{\text{NP}})$	$(-0.811[0.636], 0.128[0.273])$	3.689	36.0
S - VIII	$(C_9^{\text{NP}} = C'_9^{\text{NP}}, C_{10}^{\text{NP}} = -C'_{10}^{\text{NP}})$	$(-1.121[-0.911], 0.302[0.365])$	5.174	51.0
S - IX	$(C_9^{\text{NP}} = C'_9^{\text{NP}}, C_{10}^{\text{NP}} = C'_{10}^{\text{NP}})$	$(-0.838[-1.077], 0.015[-0.141])$	4.032	31.0
S - X	$(C_9^{\text{NP}} = -C_{10}^{\text{NP}}, C'_9^{\text{NP}} = C'_{10}^{\text{NP}})$	$(-0.986[-0.783], 0.108[0.232])$	5.412	53.0
S - XI	$(C_9^{\text{NP}} = -C_{10}^{\text{NP}}, C'_9^{\text{NP}} = -C'_{10}^{\text{NP}})$	$(-1.008[-0.800], -0.089[0.033])$	4.922	49.0

scenarios (S-I to S-XI), the predicted 1σ range of the branching ratios of $B_c \rightarrow D_s\mu^+\mu^-$ decay mode in the $q^2 \in [1, 6]$ interval is presented in Fig. 2. In this figure, the Standard

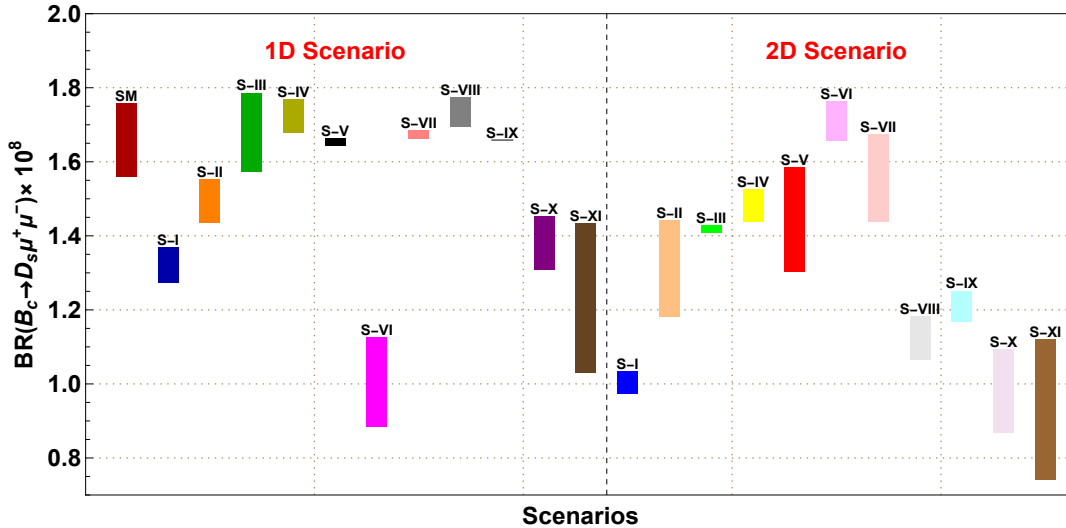


FIG. 2: Predicted range (1σ) of the branching ratio for the $B_c \rightarrow D_s\mu^+\mu^-$ process in the $q^2 \in [1, 6]$ interval for all the new physics scenarios S-I to S-XI. Left: 1D scenario; Right: 2D scenario. Here, the Standard Model prediction band reflects theoretical uncertainties.

Model result is represented in maroon color, and the prediction band reflects theoretical uncertainties, primarily arising from the form factors and CKM matrix elements. Fig. 3 depicts our predictions for the LNU parameter R_{D_s} , derived from the 1σ ranges of different 1D and 2D scenarios for the new coefficients. The numerical predictions for the branching ratio of $B_c \rightarrow D_s \mu^+ \mu^-$ and R_{D_s} in the $q^2 \in [1, 6]$ bin, using the best-fit values of all new coefficients from 1D and 2D scenarios, are presented in Table III.

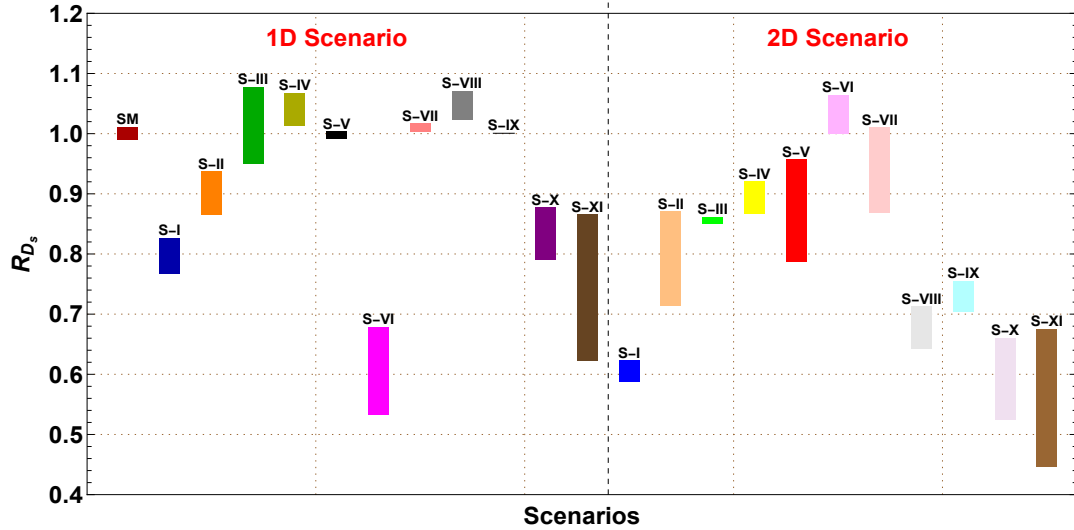


FIG. 3: Predicted range (1σ) of the lepton non-universality ratio R_{D_s} for all the new physics scenarios S-I to S-XI. Left: 1D scenario; Right: 2D scenario.

In the case of 1D scenarios, the $C_9^{\text{NP}} = -C_{10}^{\text{NP}}$ scenario is distinguishable from others by exhibiting the maximum deviation from the SM predictions. The scenarios with only C_9^{NP} , only C_{10}^{NP} , ($C_9^{\text{NP}} = -C_{10}^{\text{NP}}, C_9'^{\text{NP}} = C_{10}^{\text{NP}}$) and ($C_9^{\text{NP}} = -C_{10}^{\text{NP}} = C_9'^{\text{NP}} = -C_{10}'^{\text{NP}}$) also exhibit significant deviations from the SM results, whereas the predictions for the remaining scenarios exhibit minimal deviation or remain consistent with the Standard Model. In the low $q^2 \in [1, 6]$ GeV 2 region, R_{D_s} ratio is predicted to be less than one for the scenarios S-I, S-II, S-VI, S-X, S-XI, while predictions from other scenarios are either almost equal to or slightly greater than one.

Analysis of 2D scenarios indicates that the combinations of Wilson coefficients $(C_9^{\text{NP}}, C_{10}^{\text{NP}})$, $(C_9^{\text{NP}} = -C_{10}^{\text{NP}}, C_9'^{\text{NP}} = C_{10}^{\text{NP}})$ and $(C_9^{\text{NP}} = -C_{10}^{\text{NP}}, C_9'^{\text{NP}} = -C_{10}'^{\text{NP}})$ provide the most significant shifts from the SM results, whereas the scenario with $(C_9'^{\text{NP}}, C_{10}'^{\text{NP}})$ yields minimal deviation. With the exception of the S-VI scenario, all other scenarios predict values of the R_{D_s} parameter to be less than one.

TABLE III: Numerical predictions for the branching ratio and LNU parameter of $B_c \rightarrow D_s \mu^+ \mu^-$ using the best-fit values of new coefficients in 1D and 2D scenarios.

Scenarios	1D Scenario		2D Scenario	
	$\langle BR \rangle \times 10^8$	$\langle R_{D_s} \rangle$	$BR \times 10^8$	$\langle R_{D_s} \rangle$
SM	1.66	1.0006	1.66	1.0006
S - I	1.3	0.787	0.99	0.597
S - II	1.473	0.89	1.297	0.782
S - III	1.687	1.018	1.43	0.862
S - IV	1.71	1.036	1.433	0.864
S - V	1.66	0.9995	1.43	0.862
S - VI	0.994	0.6	1.71	1.03
S - VII	1.671	1.008	1.552	0.936
S - VIII	1.744	1.052	1.115	0.673
S - IX	1.659	1.0006	1.196	0.721
S - X	1.364	0.823	0.977	0.589
S - XI	1.253	0.756	0.92	0.555

V. INSPECTION OF $B_c \rightarrow D_s^{(*)} \mu^+ \mu^-$ DECAY

For $B_c \rightarrow D_s^{(*)} \mu^+ \mu^-$ decay, the q^2 -dependent differential decay width is given as[71]

$$\frac{d\Gamma}{dq^2} = \frac{1}{4} \left[3 I_1^c + 6 I_1^s - I_2^c - 2 I_2^s \right],$$

where $I_i^{c,s}$, the angular coefficient is described in Appendix A. In addition to examining the branching ratios, we also investigate the following observables to analyze the composition of new physical entities.

- The lepton forward-backward asymmetry:

$$A_{FB}(q^2) = \frac{3 I_6}{3 I_1^c + 6 I_1^s - I_2^c - 2 I_2^s}.$$

- The longitudinal and transverse polarization fractions of D_s^* :

$$F_L(q^2) = \frac{3 I_1^c - I_2^c}{3 I_1^c + 6 I_1^s - I_2^c - 2 I_2^s}, \quad F_T(q^2) = 1 - F_L(q^2).$$

- The Lepton Flavor Universality Violation (LFUV) ratio:

$$R_{D_s^*}(q^2) = \frac{d\Gamma(B_c \rightarrow D_s^{(*)} \mu^+ \mu^-)/dq^2}{d\Gamma(B_c \rightarrow D_s^{(*)} e^+ e^-)/dq^2}.$$

- The form factor independent (FFI) observables [72, 73]:

$$\begin{aligned} P_1 &= \frac{I_3}{2 I_2^s}, & P_2 &= \beta_l \frac{I_6^s}{8 I_2^s}, & P_3 &= -\frac{I_9}{4 I_2^s}, \\ P'_4 &= \frac{I_4}{\sqrt{-I_2^c I_2^s}}, & P'_5 &= \frac{I_5}{2 \sqrt{-I_2^c I_2^s}}, & P'_8 &= \frac{-I_8}{\sqrt{-I_2^c I_2^s}}. \end{aligned}$$

To perform the numerical analysis of $B_c \rightarrow D_s^{(*)} \mu^+ \mu^-$ channel, we use the form factors computed in the relativistic quark model from Ref. [49] and all required input parameters, such as mass, lifetime, and CKM matrix elements, from PDG site [70]. Using the 1σ range of new coefficients for both 1D and 2D scenarios, we graphically present the predicted values for various quantities related to the $B_c \rightarrow D_s^{(*)} \mu^+ \mu^-$ decay, including the branching ratio (Fig. 4), LNU parameter $R_{D_s^*}$ (Fig. 5), forward-backward asymmetry (Fig. 6) and the longitudinal polarization asymmetry (Fig. 7). The 1σ predicted values for additional

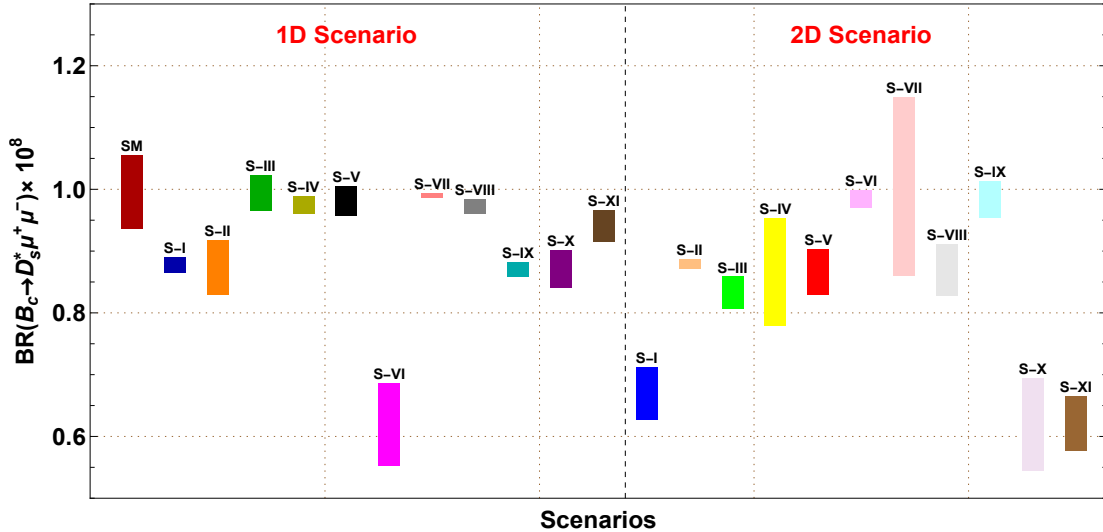


FIG. 4: Predicted 1σ range of $BR(B_c \rightarrow D_s^{(*)} \mu^+ \mu^-)$ across new physics scenarios S-I to S-XI. Left: 1D scenario; Right: 2D scenario. The range of Standard Model predictions is due to theoretical uncertainties.

clean observables, which are independent of form factors, are graphically represented in P_1 (Fig. 8), P_2 (Fig. 9), P_3 (Fig. 10), P'_4 (Fig. 11), P'_5 (Fig. 12) and P'_8 (Fig. 13).

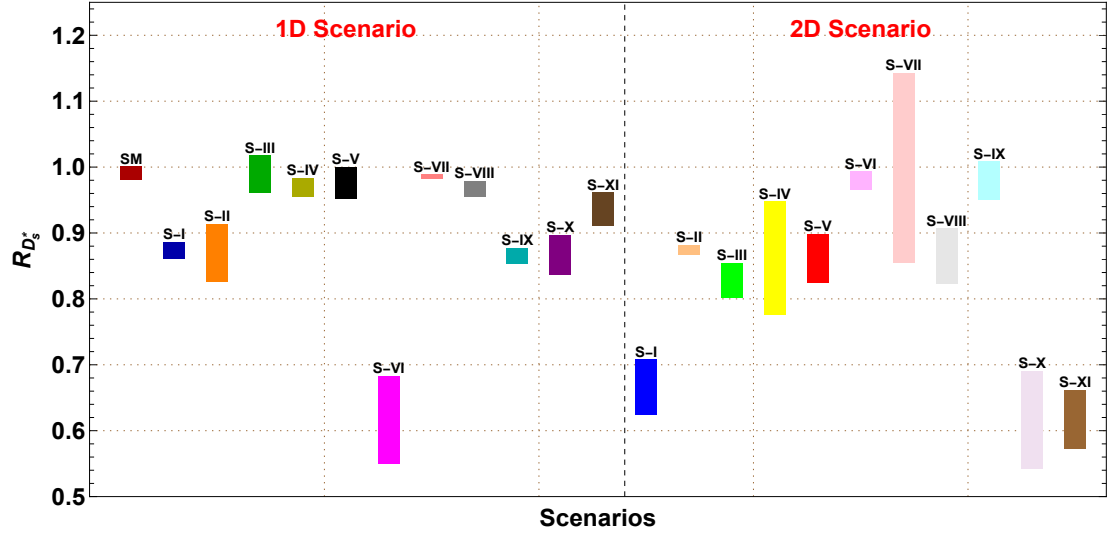


FIG. 5: Predicted 1σ range of the lepton non-universality observable $R_{D_s^*}$ within new physics scenarios S-I to S-XI. Left: 1D scenario; Right: 2D scenario.

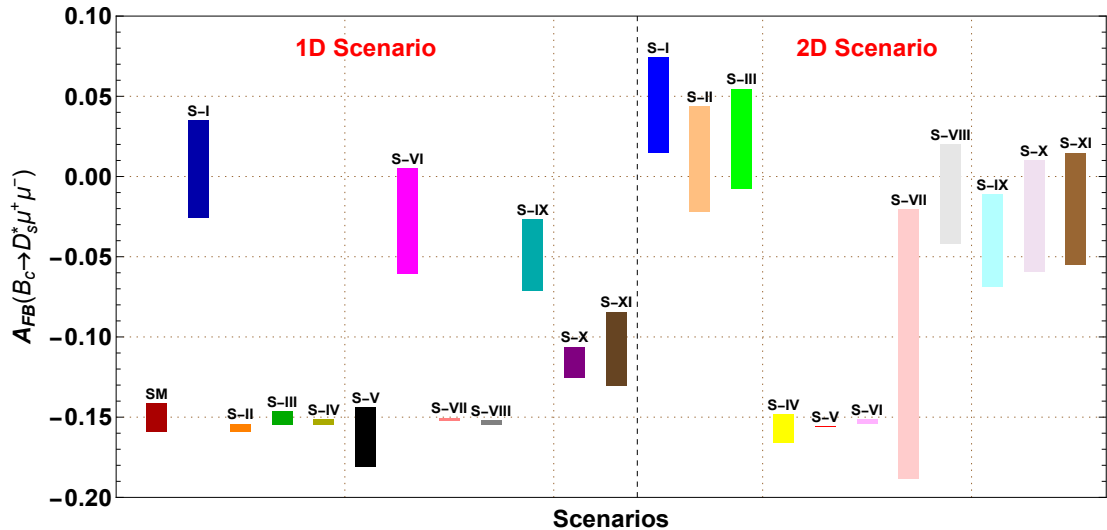


FIG. 6: Predicted range (1σ) of forward-backward asymmetry of $B_c \rightarrow D_s^{(*)} \mu^+ \mu^-$ process for all the new physics scenarios. Left: 1D scenario; Right: 2D scenario.

In these figures, the maroon color band stands for the SM prediction, which accounts for theoretical uncertainties, while the other colored bands illustrate the 1σ range of predictions based on the new coefficients. The numerical values of the branching ratios, LFUV ratio $R_{D_s^*}$, forward-backward asymmetry, longitudinal and transverse polarization asymmetries, calculated using the best-fit values of the new coefficients for both 1D and 2D scenarios, are provided in Table IV. Table V displays the numerical values of the FFI observables $P_{1,2,3}$ and

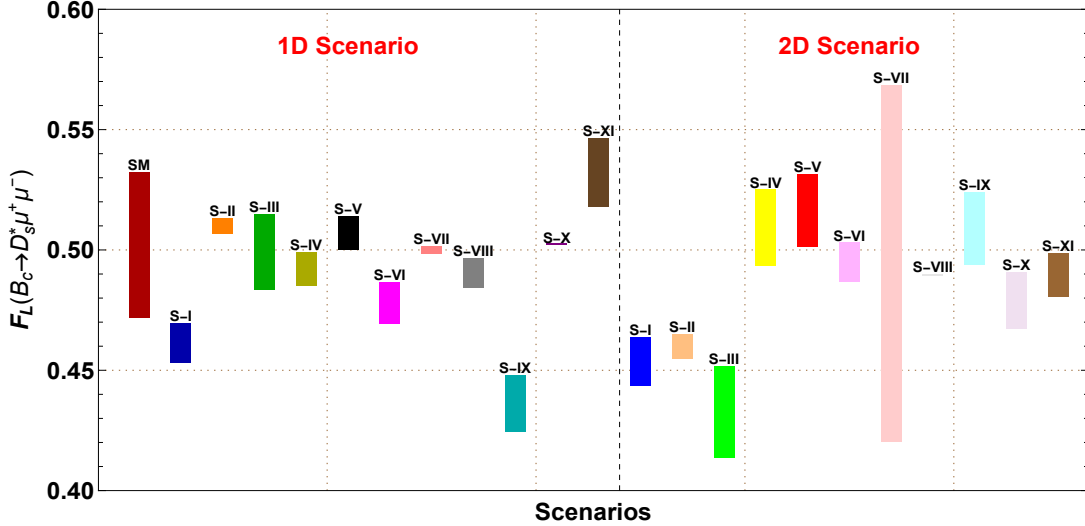


FIG. 7: Predicted range (1σ) of longitudinal polarization fraction of $B_c \rightarrow D_s^{(*)} \mu^+ \mu^-$ process for all the new physics scenarios. Left: 1D scenario; Right: 2D scenario.

$P'_{4,5,8}$, estimated using the best-fit values of the 1D and 2D coefficients. Due to the marginal effects of the new coefficients on the P'_6 observable, we did not include it in our analysis.

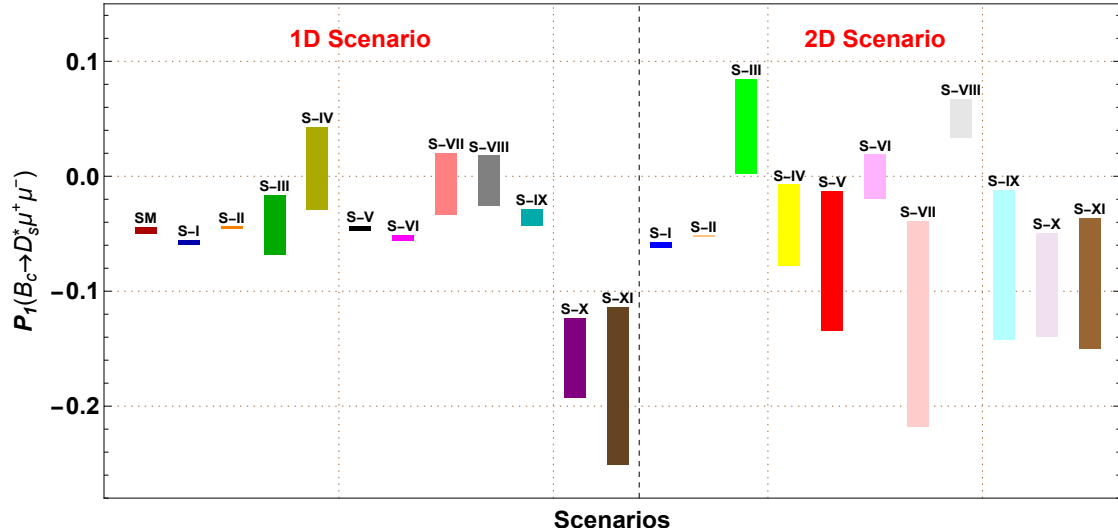


FIG. 8: Predicted range (1σ) of P_1 observable for all the new physics scenarios.
 Left: 1D scenario; Right: 2D scenario.

Within the frameworks of 1D scenarios:

- The scenario S-VI, where $C_9^{\text{NP}} = -C_{10}^{\text{NP}}$ exhibits the maximum shift in the branching ratio for $B_c \rightarrow D_s^{(*)} \mu^+ \mu^-$ in the low q^2 bin, while other scenarios show only marginal

TABLE IV: Numerical predictions for branching ratios and other physical observables of $B_c \rightarrow D_s^{(*)} \mu^+ \mu^-$ decay with 1D and 2D scenarios.

1D Scenario					
Scenarios	$BR \times 10^8$	$\langle R_{D_s^*} \rangle$	$\langle A_{FB} \rangle$	$\langle F_L \rangle$	$\langle F_T \rangle$
SM	0.996	0.991	-0.15	0.502	0.498
S - I	0.872	0.868	0.0141	0.459	0.541
S - II	0.858	0.854	-0.157	0.511	0.489
S - III	0.988	0.983	-0.151	0.498	0.502
S - IV	0.976	0.971	-0.153	0.493	0.507
S - V	0.992	0.987	-0.153	0.503	0.497
S - VI	0.613	0.61	-0.028	0.479	0.521
S - VII	0.99	0.985	-0.151	0.50	0.50
S - VIII	0.969	0.965	-0.154	0.489	0.511
S - IX	0.866	0.861	-0.046	0.434	0.566
S - X	0.863	0.859	-0.113	0.502	0.498
S - XI	0.943	0.938	-0.111	0.531	0.469
2D Scenarios					
Scenario	$BR \times 10^8$	$\langle R_{D_s^*} \rangle$	$\langle A_{FB} \rangle$	$\langle F_L \rangle$	$\langle F_T \rangle$
SM	0.996	0.991	-0.15	0.502	0.498
S - I	0.659	0.656	0.045	0.453	0.547
S - II	0.877	0.872	0.011	0.462	0.538
S - III	0.826	0.822	0.023	0.430	0.570
S - IV	0.846	0.842	-0.157	0.515	0.485
S - V	0.869	0.864	-0.156	0.518	0.482
S - VI	0.979	0.975	-0.152	0.495	0.505
S - VII	0.847	0.843	-0.053	0.446	0.554
S - VIII	0.858	0.854	-0.011	0.489	0.511
S - IX	0.981	0.976	-0.039	0.510	0.490
S - X	0.615	0.612	-0.026	0.481	0.519
S - XI	0.618	0.615	-0.021	0.490	0.510

TABLE V: Numerical predictions for form factor independent observables of
 $B_c \rightarrow D_s^{(*)} \mu^+ \mu^-$ channel with 1D and 2D scenarios.

1D Scenario						
Scenarios	$\langle P_1 \rangle$	$\langle P_2 \rangle$	$\langle P_3 \rangle \times 10^3$	$\langle P'_4 \rangle$	$\langle P'_5 \rangle$	$\langle P'_8 \rangle \times 10^2$
SM	-0.047	-0.20189	-0.289	0.433	-0.665	-0.362
S - I	-0.058	0.016	-0.304	0.426	-0.325	-0.413
S - II	-0.045	-0.215	-0.342	0.421	-0.698	-0.421
S - III	-0.04	-0.201	-0.435	0.431	-0.67	-0.34
S - IV	0.0006	-0.201	-0.29	0.42	-0.689	-0.37
S - V	-0.047	-0.206	-0.291	0.433	-0.671	-0.364
S - VI	-0.054	-0.037	-0.45	0.39	-0.47	-0.59
S - VII	-0.011	-0.202	-0.05	0.424	-0.681	-0.41
S - VIII	0.001	-0.2	-0.483	0.419	-0.691	-0.338
S - IX	-0.035	-0.055	-1.794	0.422	-0.47	-0.121
S - X	-0.165	-0.153	-1.101	0.45	-0.559	-0.285
S - XI	-0.174	-0.159	0.235	0.458	-0.546	-0.475
2D Scenarios						
Scenarios	$\langle P_1 \rangle$	$\langle P_2 \rangle$	$\langle P_3 \rangle \times 10^3$	$\langle P'_4 \rangle$	$\langle P'_5 \rangle$	$\langle P'_8 \rangle \times 10^2$
SM	-0.047	-0.2	-0.289	0.433	-0.665	-0.362
S - I	-0.06	0.054	-0.399	0.4	-0.299	-0.55
S - II	-0.058	0.013	-0.205	0.426	-0.33	-0.043
S - III	0.055	0.026	-0.305	0.392	-0.358	-0.439
S - IV	-0.049	-0.217	-0.243	0.421	-0.698	-0.446
S - V	-0.083	-0.216	-0.343	0.431	-0.678	-0.416
S - VI	-0.003	-0.202	-0.231	0.421	-0.687	-0.379
S - VII	-0.08	-0.065	-1.83	0.43	-0.471	-0.132
S - VIII	0.055	-0.016	1.93	0.395	-0.397	-0.821
S - IX	-0.08	-0.054	1.24	0.438	-0.407	-0.629
S - X	-0.099	-0.035	-0.749	0.402	-0.448	-0.534
S - XI	-0.094	-0.029	-0.207	0.4	-0.434	-0.63

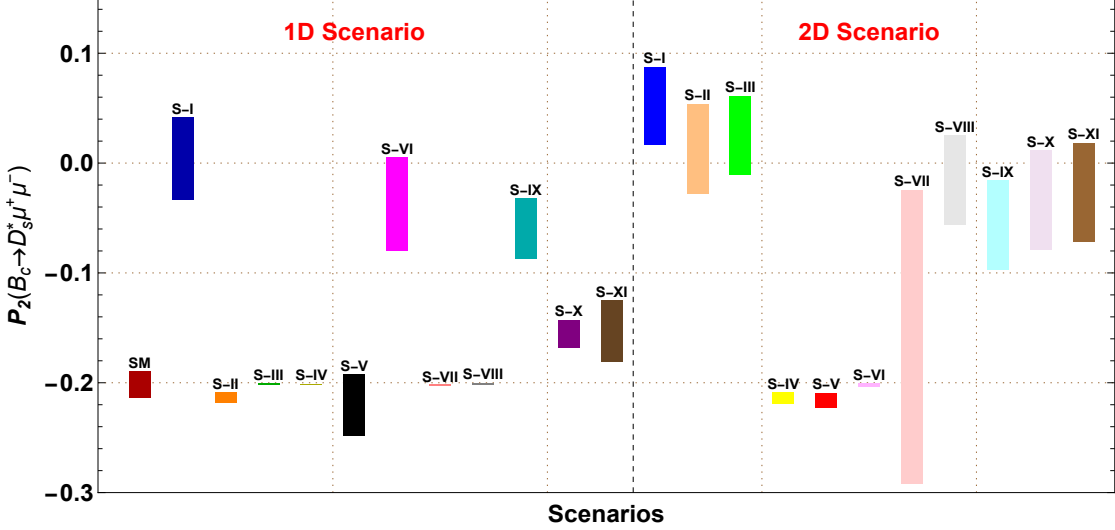


FIG. 9: Predicted range (1σ) of P_2 observable for all the new physics scenarios.

Left: 1D scenario; Right: 2D scenario.

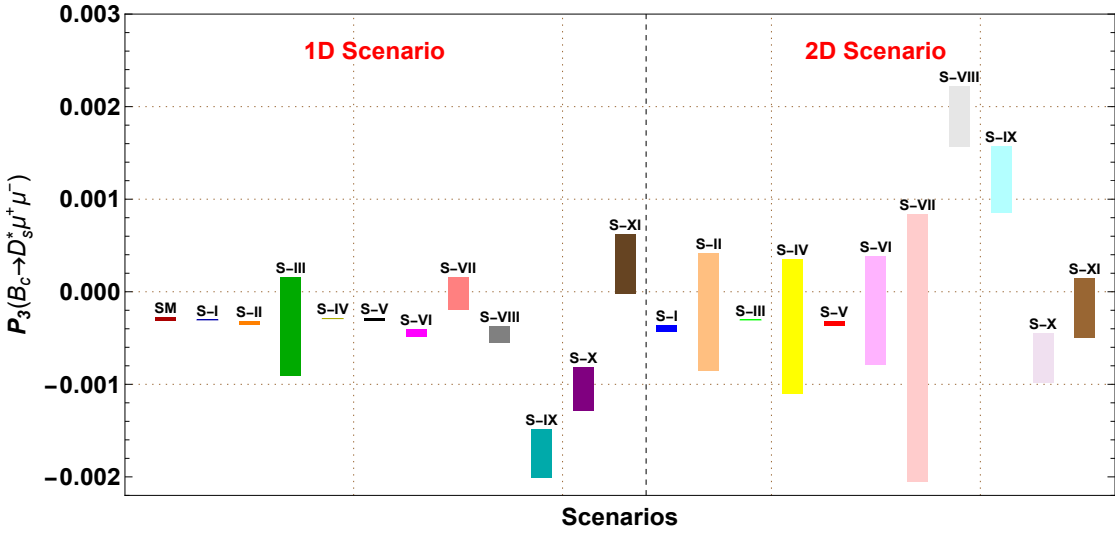


FIG. 10: Predicted range (1σ) of P_3 observable for all the new physics scenarios.

Left: 1D scenario; Right: 2D scenario.

deviations from the Standard Model prediction.

- All the scenarios predict $R_{D_s^*} < 1$, suggesting the presence of lepton flavor universality violation in $b \rightarrow s\mu^+\mu^-$ transition. Among these, the scenario with $C_9^{\text{NP}} = -C_{10}^{\text{NP}}$ shows the largest deviation from one, thereby supporting lepton non-universality.
- For the forward backward asymmetry observable, significant deviations from the SM

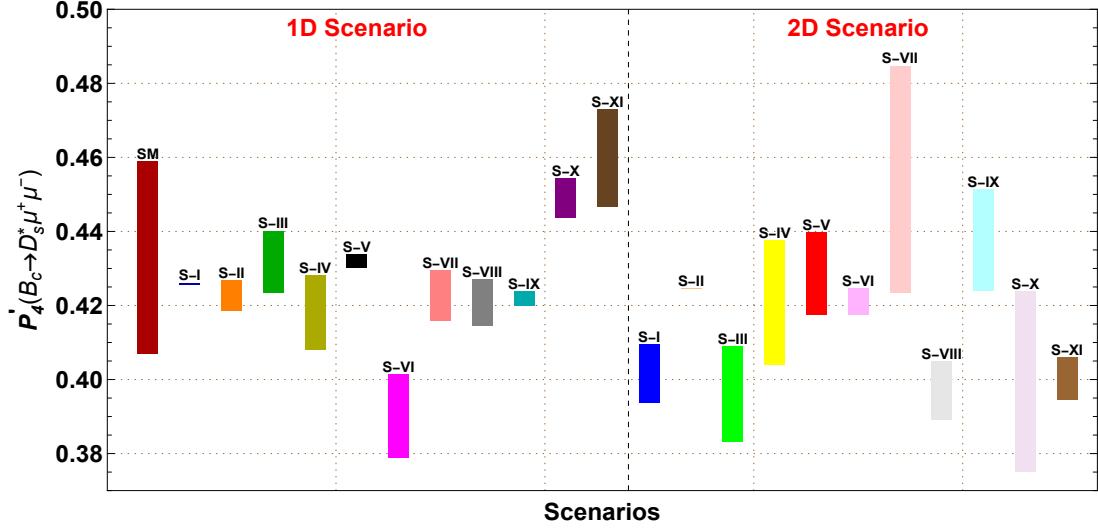


FIG. 11: Predicted range (1σ) of P'_4 observable for all the new physics scenarios.

Left: 1D scenario; Right: 2D scenario.

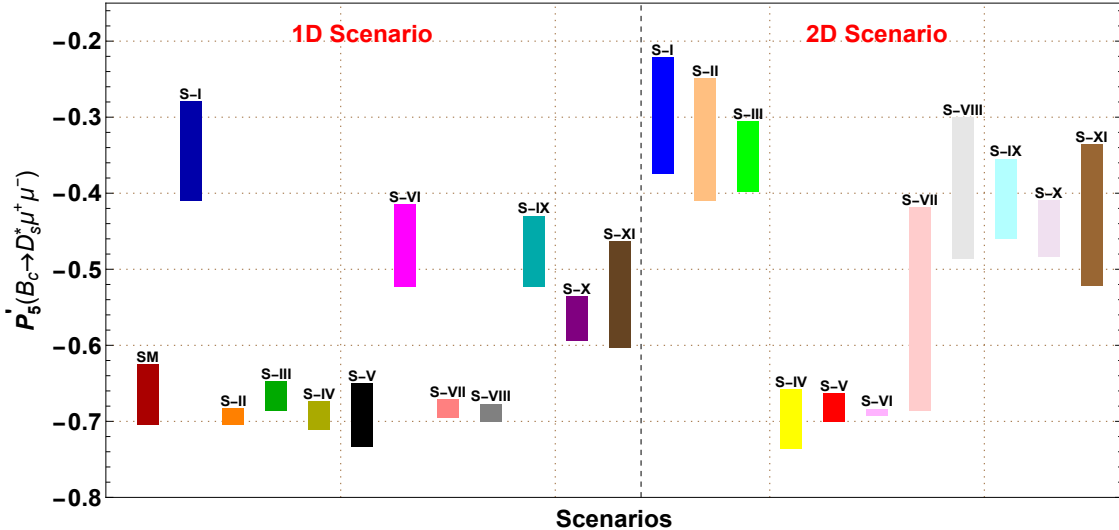


FIG. 12: Predicted range (1σ) of P'_5 observable for all the new physics scenarios.

Left: 1D scenario; Right: 2D scenario.

are observed for scenarios with only C_9^{NP} , $C_9^{\text{NP}} = -C_{10}^{\text{NP}}$ and $C_9^{\text{NP}} = -C_9'^{\text{NP}}$ coefficients.

- The prediction for longitudinal polarization asymmetry with $C_9^{\text{NP}} = -C_9'^{\text{NP}}$ shows the comparatively large deviation from the Standard Model result than other scenarios.
- In the analysis of form factor independent clean observables in the low q^2 bin, we observe that:

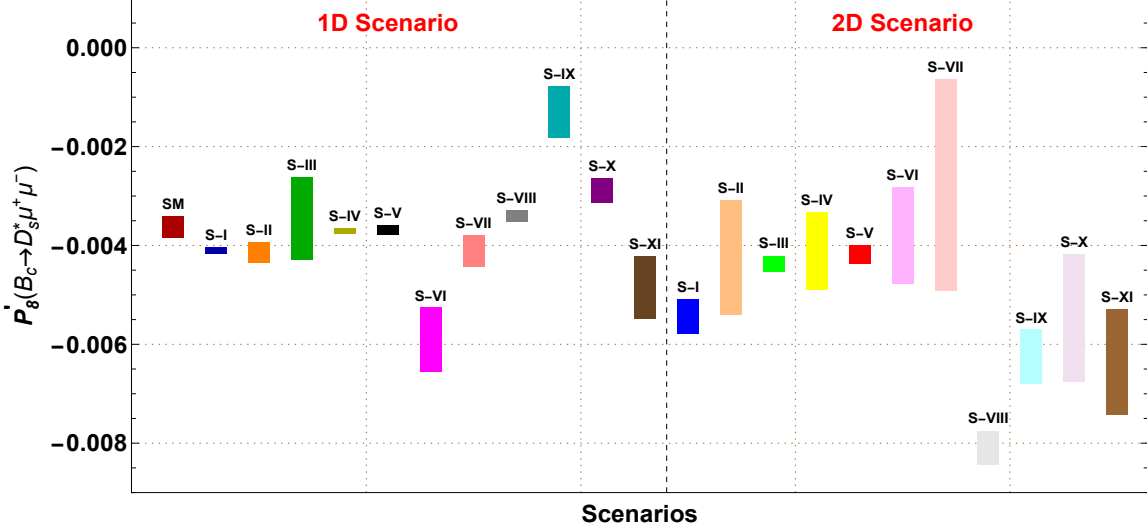


FIG. 13: Predicted range (1σ) of P'_8 observable for all the new physics scenarios.

Left: 1D scenario; Right: 2D scenario.

- (i) Scenarios S-X and S-XI are particularly sensitive to the P_1 observable,
- (ii) The P_2 observable shows maximum deviations for scenarios S-I, S-VI and S-IX,
- (iii) The P_3 observable deviates most significantly for the S-IX scenario,
- (iv) The S-VI scenario scenario has a notable impact on the P'_4 observable,
- (v) The P'_5 observable receives the maximum contribution from scenarios S-I, S-VI and S-IX scenarios,
- (vi) Scenarios S-VI and S-IX are crucial for the P'_8 observable.

In the realm of 2D scenarios:

- The branching ratio of $B_c \rightarrow D_s^{(*)}\mu^+\mu^-$ differs significantly for the new scenarios S-I, S-X and S-XI.
- All scenarios predict that the $R_{D_s^*}$ ratio is less than one. Scenarios S-I, S-X and S-XI show the greatest deviations from one, suggesting the possibility of lepton universality violation in the $b \rightarrow s\mu^+\mu^-$ decay mode.
- With the exception of scenarios S-IV, S-V and S-VI, all other scenarios make significant contributions to the forward-backward asymmetry of the $B_c \rightarrow D_s^{(*)}\mu^+\mu^-$ decay mode in the low q^2 region.

- All the scenarios have marginal deviation from the SM prediction of the longitudinal polarization asymmetry.
- The S-III scenario exhibits a comparatively larger deviation for the P_1 observable.
- With the exception of S-IV, S-V, and S-VI, all other scenarios show significant deviations from the Standard Model prediction of P_2 observable. The S-VII scenario has an overlap region with the SM band.
- The S-VIII and S-IX scenarios display maximum sensitivity to the P_3 observable.
- Apart from the S-VIII and S-XI scenarios, the predicted 1σ bands of all other scenarios overlap with the SM band for the P'_4 observable.
- Except for S-IV, S-V, and S-VI, all other scenarios show significant deviations from the SM predictions for P'_5 .
- The S-VIII scenario is particularly sensitive to the P'_8 observable.

VI. CONCLUSION

In this work, we investigated the sensitivity of (axial)vector coefficients on the $B_c \rightarrow D_s^{(*)}\mu^+\mu^-$ decay mode in the low $q^2 \in [1, 6]$ GeV 2 bin. For this analysis, we updated the allowed ranges for various 1D and 2D coefficients using the latest data on the $b \rightarrow s\mu^+\mu^-$ transition, utilizing the `flavio` package. Due to minimal variation between theoretical and experimental predictions for R_{K^*} , we did not include these ratios in our analysis. Based on the 1σ range of 1D and 2D solutions, we estimated the 1σ predicted values for the branching ratio and lepton non-universality parameter of the $B_c \rightarrow D_s^{(*)}\mu^+\mu^-$ process. Additionally, we analyzed the forward-backward asymmetry, longitudinal and transverse polarization asymmetries, and form factor-independent observables for the $B_c \rightarrow D_s^{(*)}\mu^+\mu^-$ decay across both scenarios.

Within the framework of 1D scenarios, the coefficients $C_9^{\text{NP}} = -C_{10}^{\text{NP}}$ and $C_9'^{\text{NP}}$ provide a good fit to the $b \rightarrow s\mu^+\mu^-$ and exhibit significant deviations from the Standard Model predictions for all observables in the $B_c \rightarrow D_s^{(*)}\mu^+\mu^-$ decay process. These scenarios also predict $R_{D_s^{(*)}}$ values below one, suggesting potential lepton flavor universality violation in

the $b \rightarrow s\mu^+\mu^-$ transition, despite the consistent results for $R_{K^{(*)}}$ reported by the LHCb Collaboration.

From the perspective of 2D scenarios, we observed that the new Wilson coefficient combinations $(C_9^{\text{NP}}, C_{10}^{\text{NP}})$, $(C_9^{\text{NP}}, C'^{\text{NP}}_{10})$, $(C_9^{\text{NP}} = C'^{\text{NP}}_9, C_{10}^{\text{NP}} = -C'^{\text{NP}}_{10})$ and $(C_9^{\text{NP}} = -C_{10}^{\text{NP}}, C'_9 = C'^{\text{NP}}_{10})$ provide an excellent fit to all observables in the $b \rightarrow s\mu^+\mu^-$ very well. These 2D scenarios are particularly notable for their sensitivity to the observables of $B_c \rightarrow D_s^{(*)}\mu^+\mu^-$ and exhibit significant deviations from the Standard Model predictions.

In conclusion, a thorough analysis of the discussed 1D and 2D scenarios has the potential to address the major B anomalies and confirm the existence of lepton non-universality in the $b \rightarrow s\mu^+\mu^-$ transition. Moreover, detailed investigations and searches for $B_c \rightarrow D_s^{(*)}\mu^+\mu^-$ decay modes could provide valuable insights into the presence of new physics.

Acknowledgment

AKY expresses gratitude to the DST-Inspire Fellowship division, Government of India, for financial support under ID No. IF210687. MKM would like to acknowledge the financial support from the IoE PDRF at the University of Hyderabad. Additionally, MKM extends sincere thanks to Dr. Jacky Kumar and Dr. Girish Kumar for their valuable suggestions regarding the flavio package.

Appendix A: The angular coefficient I_i

The angular coefficients I_i as a functions of the transversity amplitudes are defined as [58, 66, 74, 75]

$$\begin{aligned}
I_1^c &= \left(|A_L^0|^2 + |A_R^0|^2 \right) + 8 \frac{m_l^2}{q^2} \operatorname{Re} \left[A_L^0 A_R^{0*} \right] + 4 \frac{m_l^2}{q^2} |A_t|^2, \\
I_2^c &= -\beta_l^2 \left(|A_L^0|^2 + |A_R^0|^2 \right), \\
I_1^s &= \frac{(2 + \beta_l^2)}{4} \left[|A_L^\perp|^2 + |A_L^{\parallel}|^2 + |A_R^\perp|^2 + |A_R^{\parallel}|^2 \right] + \frac{4m_l^2}{q^2} \operatorname{Re} \left[A_L^\perp A_R^{\perp*} + A_L^{\parallel} A_R^{\parallel*} \right], \\
I_2^s &= \frac{1}{4} \beta_l^2 \left[|A_L^\perp|^2 + |A_L^{\parallel}|^2 + |A_R^\perp|^2 + |A_R^{\parallel}|^2 \right], \\
I_3 &= \frac{1}{2} \beta_l^2 \left[|A_L^\perp|^2 - |A_L^{\parallel}|^2 + |A_R^\perp|^2 - |A_R^{\parallel}|^2 \right], \\
I_4 &= \frac{1}{\sqrt{2}} \beta_l^2 \left[\operatorname{Re} \left(A_L^0 A_L^{\parallel*} \right) + \operatorname{Re} \left(A_R^0 A_R^{\parallel*} \right) \right], \\
I_5 &= \sqrt{2} \beta_l \left[\operatorname{Re} \left(A_L^0 A_L^{\perp*} \right) - \operatorname{Re} \left(A_R^0 A_R^{\perp*} \right) \right], \\
I_6 &= 2 \beta_l \left[\operatorname{Re} \left(A_L^{\parallel} A_L^{\perp*} \right) - \operatorname{Re} \left(A_R^{\parallel} A_R^{\perp*} \right) \right], \\
I_7 &= \sqrt{2} \beta_l \left[\operatorname{Im} \left(A_L^0 A_L^{\parallel*} \right) - \operatorname{Im} \left(A_R^0 A_R^{\parallel*} \right) \right], \\
I_8 &= \frac{1}{\sqrt{2}} \beta_l^2 \left[\operatorname{Im} \left(A_L^0 A_L^{\perp*} \right) + \operatorname{Im} \left(A_R^0 A_R^{\perp*} \right) \right], \\
I_9 &= \beta_l^2 \left[\operatorname{Im} \left(A_L^{\parallel} A_L^{\perp*} \right) + \operatorname{Im} \left(A_R^{\parallel} A_R^{\perp*} \right) \right],
\end{aligned}$$

where the transversity amplitude, $A_{R,L}^{\perp,\parallel,0}$ in terms of form factors are given by [58]

$$\begin{aligned}
A_{R,L}^0 &= N_{D_s^*} \frac{1}{2 m_{D_s^*} \sqrt{q^2}} \left[(C_9^{eff} \pm C_{10}) \left[(m_{B_c}^2 - m_{D_s^*}^2 - q^2)(m_{B_c} + m_{D_s^*}) A_1 - \frac{\lambda(m_{B_c}^2, m_{D_s^*}^2, q^2)}{m_{B_c} + m_{D_s^*}} A_2 \right] \right. \\
&\quad \left. + 2m_b C_7^{eff} \left[(m_{B_c}^2 + 3m_{D_s^*}^2 - q^2) T_2 - \frac{\lambda(m_{B_c}^2, m_{D_s^*}^2, q^2)}{m_{B_c}^2 - m_{D_s^*}^2} T_3 \right] \right]; \\
A_{R,L}^\perp &= -N_{D_s^*} \sqrt{2} \left[(C_9^{eff} \pm C_{10}) \frac{\sqrt{\lambda(m_{B_c}^2, m_{D_s^*}^2, q^2)}}{m_{B_c} + m_{D_s^*}} V + \frac{\sqrt{\lambda(m_{B_c}^2, m_{D_s^*}^2, q^2)} 2m_b C_7^{eff}}{q^2} T_1 \right]; \\
A_{R,L}^{\parallel} &= N_{D_s^*} \sqrt{2} \left[(C_9^{eff} \pm C_{10})(m_{B_c} + m_{D_s^*}) A_1 + \frac{2m_b C_7^{eff} (m_{B_c}^2 - m_{D_s^*}^2)}{q^2} T_2 \right]; \\
A_{R,L}^t &= N_{D_s^*} (C_9^{eff} \pm C_{10}) \frac{\sqrt{\lambda(m_{B_c}^2, m_{D_s^*}^2, q^2)}}{\sqrt{q^2}} A_0;
\end{aligned}$$

with

$$N_{D_s^*} = \left[\frac{G_F^2 \alpha_e^2}{3.2^{10} \pi^5 m_{B_c}^3} |V_{tb} V_{ts}^*|^2 q^2 \sqrt{\lambda(m_{B_c}^2, m_{D_s^*}^2, q^2)} \left[1 - \frac{4m_l^2}{q^2} \right]^{1/2} \right]^{1/2}.$$

The detailed expressions for the form factors $(V, A_0, A_1, T_1, T_2, T_3)$ for $B_c \rightarrow D_s^{(*)}$ in the relativistic quark model are provided in the Ref. [49, 50].

- [1] R. Aaij *et al.* (LHCb), **JHEP** **02**, 104 (2016), arXiv:1512.04442 [hep-ex] .
- [2] R. Aaij *et al.* (LHCb), **JHEP** **12**, 081 (2020), arXiv:2010.06011 [hep-ex] .
- [3] R. Aaij *et al.* (LHCb), **Phys. Rev. Lett.** **126**, 161802 (2021), arXiv:2012.13241 [hep-ex] .
- [4] R. Aaij *et al.* (LHCb), **Phys. Rev. Lett.** **125**, 011802 (2020), arXiv:2003.04831 [hep-ex] .
- [5] R. e. a. L. C. Aaij (LHCb Collaboration), **Phys. Rev. Lett.** **131**, 051803 (2023).
- [6] Belle II Collaboration, A. Glazov, “News from Belle II,” (EPS conference 2023).
- [7] R. Aaij *et al.* (LHCb), **JHEP** **02**, 032 (2024), arXiv:2308.06162 [hep-ex] .
- [8] B. Capdevila, A. Crivellin, and J. Matias, **Eur. Phys. J. ST** **1**, 20 (2023), arXiv:2309.01311 [hep-ph] .
- [9] S. Sahoo and R. Mohanta, **J. Phys. G** **44**, 035001 (2017), arXiv:1612.02543 [hep-ph] .
- [10] T. Hurth, F. Mahmoudi, and S. Neshatpour, **Phys. Rev. D** **108**, 115037 (2023), arXiv:2310.05585 [hep-ph] .
- [11] F. Mahmoudi and Y. Monceaux, **Symmetry** **16**, 1006 (2024), arXiv:2408.03235 [hep-ph] .
- [12] N. Rajeev, N. Sahoo, and R. Dutta, **Phys. Rev. D** **103**, 095007 (2021), arXiv:2009.06213 [hep-ph] .
- [13] N. Rajeev and R. Dutta, **Phys. Rev. D** **105**, 115028 (2022), arXiv:2112.11682 [hep-ph] .
- [14] M. K. Mohapatra and A. Giri, **Phys. Rev. D** **104**, 095012 (2021), arXiv:2109.12382 [hep-ph] .
- [15] N. Das and R. Dutta, **Phys. Rev. D** **108**, 095051 (2023), arXiv:2307.03615 [hep-ph] .
- [16] A. K. Yadav, M. K. Mohapatra, and S. Sahoo, in *22nd Conference on Flavor Physics and CP Violation* (2024) arXiv:2408.16439 [hep-ph] .
- [17] R. Aaij *et al.* (LHCb), **Phys. Rev. Lett.** **115**, 111803 (2015), [Erratum: **Phys. Rev. Lett.** **115**, 159901 (2015)], arXiv:1506.08614 [hep-ex] .
- [18] R. Aaij *et al.* (LHCb), **Phys. Rev. Lett.** **120**, 121801 (2018), arXiv:1711.05623 [hep-ex] .
- [19] J. P. Lees *et al.* (BaBar), **Phys. Rev. Lett.** **109**, 101802 (2012), arXiv:1205.5442 [hep-ex] .
- [20] J. P. Lees *et al.* (BaBar), **Phys. Rev. D** **88**, 072012 (2013), arXiv:1303.0571 [hep-ex] .
- [21] M. Huschle *et al.* (Belle), **Phys. Rev. D** **92**, 072014 (2015), arXiv:1507.03233 [hep-ex] .
- [22] A. Abdesselam *et al.* (Belle), (2019), arXiv:1904.08794 [hep-ex] .

- [23] Y. Sato *et al.* (Belle), Phys. Rev. D **94**, 072007 (2016), arXiv:1607.07923 [hep-ex] .
- [24] I. Adachi *et al.* (Belle-II), (2024), arXiv:2401.02840 [hep-ex] .
- [25] S. Sahoo, R. Mohanta, and A. K. Giri, Phys. Rev. D **95**, 035027 (2017), arXiv:1609.04367 [hep-ph] .
- [26] R. Aaij *et al.* (LHCb), Phys. Rev. Lett. **131**, 111802 (2023), arXiv:2302.02886 [hep-ex] .
- [27] R. Aaij *et al.* (LHCb), Phys. Rev. D **108**, 012018 (2023), [Erratum: Phys.Rev.D 109, 119902 (2024)], arXiv:2305.01463 [hep-ex] .
- [28] A. Mathad (LHCb), in *57th Rencontres de Moriond on Electroweak Interactions and Unified Theories* (2023) arXiv:2305.08133 [hep-ex] .
- [29] J. Harrison and C. T. H. Davies (HPQCD, (HPQCD Collaboration)‡), Phys. Rev. D **109**, 094515 (2024), arXiv:2304.03137 [hep-lat] .
- [30] *Test of lepton flavor universality in $B^\pm \rightarrow K^\pm \ell^+ \ell^-$ decays*, Tech. Rep. (CERN, Geneva, 2023).
- [31] A. M. Sirunyan *et al.* (CMS), Phys. Lett. B **781**, 517 (2018), arXiv:1710.02846 [hep-ex] .
- [32] S. Wehle *et al.* (Belle), Phys. Rev. Lett. **118**, 111801 (2017), arXiv:1612.05014 [hep-ex] .
- [33] M. Aaboud *et al.* (ATLAS), JHEP **10**, 047 (2018), arXiv:1805.04000 [hep-ex] .
- [34] *Angular analysis of the $B^0 \rightarrow K^{*0}(892)\mu^+\mu^-$ decay at $\sqrt{s} = 13$ TeV*, Tech. Rep. (CERN, Geneva, 2024).
- [35] R. Aaij *et al.* (LHCb), JHEP **07**, 084 (2013), arXiv:1305.2168 [hep-ex] .
- [36] N. Gubernari, D. van Dyk, and J. Virto, JHEP **02**, 088 (2021), arXiv:2011.09813 [hep-ph] .
- [37] R. Aaij *et al.* (LHCb), JHEP **09**, 179 (2015), arXiv:1506.08777 [hep-ex] .
- [38] R. Aaij *et al.* (LHCb), Phys. Rev. Lett. **127**, 151801 (2021), arXiv:2105.14007 [hep-ex] .
- [39] R. Aaij *et al.* (LHCb), JHEP **11**, 043 (2021), arXiv:2107.13428 [hep-ex] .
- [40] R. Aaij *et al.* (LHCb), Phys. Rev. Lett. **128**, 191802 (2022), arXiv:2110.09501 [hep-ex] .
- [41] R. Aaij *et al.* (LHCb), JHEP **08**, 055 (2017), arXiv:1705.05802 [hep-ex] .
- [42] A. Hayrapetyan *et al.* (CMS), Rept. Prog. Phys. **87**, 077802 (2024), arXiv:2401.07090 [hep-ex]
- .
- [43] M. A. Ivanov, J. G. Körner, J. N. Pandya, P. Santorelli, N. R. Soni, and C.-T. Tran, Front. Phys. (Beijing) **14**, 64401 (2019), arXiv:1904.07740 [hep-ph] .
- [44] M. A. Ivanov, J. N. Pandya, P. Santorelli, and N. R. Soni, (2024), arXiv:2404.15085 [hep-ph]
- .
- [45] H.-M. Choi, Phys. Rev. D **81**, 054003 (2010), arXiv:1001.3432 [hep-ph] .

- [46] K. Azizi, F. Falahati, V. Bashiry, and S. M. Zebarjad, *Phys. Rev. D* **77**, 114024 (2008), arXiv:0806.0583 [hep-ph].
- [47] K. Azizi and R. Khosravi, *Phys. Rev. D* **78**, 036005 (2008), arXiv:0806.0590 [hep-ph].
- [48] L. J. Cooper, C. T. H. Davies, and M. Wingate (HPQCD), *Phys. Rev. D* **105**, 014503 (2022), arXiv:2108.11242 [hep-lat].
- [49] D. Ebert, R. N. Faustov, and V. O. Galkin, *Phys. Rev. D* **82**, 034032 (2010), arXiv:1006.4231 [hep-ph].
- [50] M. Zaki, M. A. Paracha, and F. M. Bhutta, *Nucl. Phys. B* **992**, 116236 (2023), arXiv:2303.01145 [hep-ph].
- [51] M. K. Mohapatra, N. Rajeev, and R. Dutta, *Phys. Rev. D* **105**, 115022 (2022), arXiv:2108.10106 [hep-ph].
- [52] R. Dutta, *Phys. Rev. D* **100**, 075025 (2019), arXiv:1906.02412 [hep-ph].
- [53] Y.-S. Li and X. Liu, *Phys. Rev. D* **108**, 093005 (2023), arXiv:2309.08191 [hep-ph].
- [54] W.-L. Ju, G.-L. Wang, H.-F. Fu, T.-H. Wang, and Y. Jiang, *JHEP* **04**, 065 (2014), arXiv:1307.5492 [hep-ph].
- [55] A. Ahmed, I. Ahmed, M. A. Paracha, M. Junaid, A. Rehman, and M. J. Aslam (2011) arXiv:1108.1058 [hep-ph].
- [56] L.-x. Lu, Z.-j. Xiao, S.-w. Wang, and Z.-q. Zhang, *Commun. Theor. Phys.* **59**, 187 (2013), arXiv:1204.6635 [hep-ph].
- [57] A. Ali, P. Ball, L. T. Handoko, and G. Hiller, *Phys. Rev. D* **61**, 074024 (2000), arXiv:hep-ph/9910221 .
- [58] W. Altmannshofer, P. Ball, A. Bharucha, A. J. Buras, D. M. Straub, and M. Wick, *JHEP* **01**, 019 (2009), arXiv:0811.1214 [hep-ph].
- [59] S. Sahoo and R. Mohanta, *Phys. Rev. D* **93**, 034018 (2016), arXiv:1507.02070 [hep-ph].
- [60] A. Ali, P. Ball, L. T. Handoko, and G. Hiller, *Phys. Rev. D* **61**, 074024 (2000).
- [61] R. Aaij *et al.* (LHCb), *Phys. Rev. D* **105**, 012010 (2022), arXiv:2108.09283 [hep-ex].
- [62] ATLAS Collaboration, “ATLAS-CONF-2020-049,” (2020), <https://inspirehep.net/files/7c01a04cd7035f854c9f43648d66343b>.
- [63] M. Aaboud *et al.* (ATLAS), *JHEP* **04**, 098 (2019), arXiv:1812.03017 [hep-ex].
- [64] A. M. Sirunyan *et al.* (CMS), *JHEP* **04**, 188 (2020), arXiv:1910.12127 [hep-ex].
- [65] R. Aaij *et al.* (LHCb), *Phys. Rev. Lett.* **118**, 191801 (2017), arXiv:1703.05747 [hep-ex].

- [66] R. Aaij *et al.* (LHCb), *JHEP* **06**, 133 (2014), arXiv:1403.8044 [hep-ex] .
- [67] R. Aaij *et al.* (LHCb), *JHEP* **11**, 047 (2016), [Erratum: *JHEP* 04, 142 (2017)], arXiv:1606.04731 [hep-ex] .
- [68] D. M. Straub, (2018), arXiv:1810.08132 [hep-ph] .
- [69] C. Bobeth, G. Hiller, and G. Piranishvili, *JHEP* **12**, 040 (2007), arXiv:0709.4174 [hep-ph] .
- [70] S. Navas *et al.* (Particle Data Group), *Phys. Rev. D* **110**, 030001 (2024).
- [71] W. Altmannshofer, P. Ball, A. Bharucha, A. J. Buras, D. M. Straub, and M. Wick, *Journal of High Energy Physics* **2009**, 019–019 (2009).
- [72] S. Descotes-Genon, T. Hurth, J. Matias, and J. Virto, *Journal of High Energy Physics* **2013** (2013), 10.1007/jhep05(2013)137.
- [73] J. Matias, F. Mescia, M. Ramon, and J. Virto, *Journal of High Energy Physics* **2012** (2012), 10.1007/jhep04(2012)104.
- [74] C. Bobeth, G. Hiller, and G. Piranishvili, *Journal of High Energy Physics* **2008**, 106–106 (2008).
- [75] F. Kruger and J. Matias, *Phys. Rev. D* **71**, 094009 (2005), arXiv:hep-ph/0502060 .